62 *Inorg. Chem.* **2011**, *50*, 62–71
DOI: 10.1021/ic1010874

Inorganic Chemistry
Article

Borylene-Based Functionalization of Iron-Alkynyl-σ-Complexes and Stepwise Reversible Metal-Boryl-to-Borirene Transformation: Synthesis, Characterization, and Density Functional Theory Studies

Holger Braunschweig,* Qing Ye, Krzysztof Radacki, and Peter Brenner

Institut für Anorganische Chemie, Bayerische Julius-Maximilians-Universität Würzburg Am Hubland, 97 074 Würzburg, Germany

Gernot Frenking* and Susmita De

Fachbereich Chemie, Philipps-Universität Marburg Hans-Meerwein-Strasse, 35043 Marburg, Germany

Received June 1, 2010

Thermally induced chemoselective borylene transfer from $[(OC)_5Mo{=}BN(SiMe_3)_2]$ (**2a**) to the carbon−carbon triple bond of an iron dicarbonyl alkynyl complex $[(\eta^5\text{-}C_5Me_5)Fe(CO)_2C{\equiv}CPh]$ (**3**) led to the isolation of an iron aminoborirene complex $[(\eta^5\text{-}C_5Me_5)(OC)_2Fe\{\mu\text{-}BN(SiMe_3)_2C{=}C\}Ph]$ (**4**) in satisfactory yield. Room temperature photolysis of **4** resulted in an unprecedented rearrangement and a concurrent decarbonylation, affording the novel C_2 side-on coordinated iron boryl complex $[(\eta^5\text{-}C_5Me_5)(OC)FeBN(SiMe_3)_2(\eta^2\text{-}CC)Ph]$ (**5**). Carbonylation of **5** under CO atmosphere at ambient temperature yielded $[(\eta^5\text{-}C_5Me_5)(OC)_2FeBN(SiMe_3)_2CCPh]$ (**6**), which is an isomer of **4**. Decarbonylation of **6** at 80 °C led to **5**, which could be upon introduction of CO gas further converted into **4** under same conditions. Reaction of **5** with PMe_3 at 80 °C yielded the phosphane complex $[(\eta^5\text{-}C_5Me_5)(OC)(PMe_3)Fe\{\mu\text{-}BN(SiMe_3)_2C{=}C\}Ph]$ (**7**). All above-mentioned iron complexes **4**−**7** were isolated as air and moisture sensitive crystalline solids in good yields and have been fully characterized in solution and by X-ray crystallography. Quantum chemical calculations using density functional theory (DFT) have been carried out to understand the mechanisms of the experimentally observed reactions and to analyze the bonding situation in the molecules **4**−**7**.

Introduction

Free borylenes of the general type ":B-R" constitute hypovalent, highly reactive species that can only be obtained by applying drastic conditions as shown by Timms et al. in the case of flouroborylene ":B−F" already in the 1960s.[1] Likewise, in 1984, West et al. published the photochemical generation of the silylborylene ":B-$SiPh_3$" in hydrocarbon matrixes at −196 °C and a number of well characterized trapping products derived thereof.[2] During the past decade borylene chemistry has been put into focus again, as it became possible to generate and stabilize borylenes as ligands in the coordination sphere of various transition metals under standard conditions.[3]

The ligand properties of borylenes have been closely studied, in particular by computational methods,[4,5] thus revealing a close relationship to the isolectronic carbonyls in terms of bonding pattern and coordination modes. However,

*To whom correspondence should be addressed. E-mail: h.braunschweig@mail.uni-wuerzburg.de (H.B.); frenking@see.foot.note (G.F.). Fax: (+49) 931-888-4623 (H.B.); +49-(0)6421-28-25566 (G.F.).

(1) (a) Timms, P. L. *J. Am. Chem. Soc.* **1967**, *89*, 1629. (b) Timms, P. L. *Acc. Chem. Res.* **1973**, *6*, 118.

(2) Pachaly, B.; West, R. *Angew. Chem.* **1984**, *96*, 444. Pachaly, B.; West, R. *Angew. Chem., Int. Ed. Engl.* **1984**, *23*, 454.

(3) (a) Braunschweig, H. *Angew. Chem.* **1998**, *110*, 1882. Braunschweig, H. *Angew. Chem., Int. Ed.* **1998**, *37*, 1786. (b) Wrackmeyer, B. *Angew. Chem.* **1999**, *111*, 817. Wrackmeyer, B. *Angew. Chem., Int. Ed.* **1999**, *38*, 771. (c) Braunschweig, H.; Colling, M. *J. Organomet. Chem.* **2000**, *18*, 614. (d) Braunschweig, H.; Colling, M. *Coord. Chem. Rev.* **2001**, *223*, 1. (e) Braunschweig, H.; Colling, M. *Eur. J. Inorg. Chem.* **2003**, 393. (f) Aldridge, S.; Coombs, D. L. *Coord. Chem. Rev.* **2004**, *248*, 535. (g) Braunschweig, H. *Adv. Organomet. Chem.* **2004**, *51*, 163. (h) Braunschweig, H.; Whittell, G. R. *Chem.—Eur. J.* **2005**, *11*, 6128. (i) Braunschweig, H.; Rais, D. *Heteroat. Chem.* **2005**, *16*, 566. (j) Braunschweig, H.; Kollann, C.; Rais, D. *Angew. Chem.* **2006**, *118*, 5380. Braunschweig, H.; Kollann, C.; Rais, D. *Angew. Chem., Int. Ed.* **2006**, *45*, 5252. (k) Anderson, C. E.; Braunschweig, H.; Dewhurst, R. D. *Organometallics* **2008**, *27*, 6381. (l) Vidovic, D.; Pierce, G. A.; Aldridge, S. *Chem. Commun.* **2009**, 1157.

(4) (a) Radius, U.; Bickelhaupt, F. M.; Ehlers, A. W.; Goldberg, N.; Hoffmann, R. *Inorg. Chem.* **1998**, *37*, 1080. (b) Macdonald, C. L. B.; Cowley, A. H. *J. Am. Chem. Soc.* **1999**, *121*, 12113. (c) Uddin, J.; Boehme, C.; Frenking, G. *Organometallics* **2000**, *19*, 571. (d) Chen, Y.; Frenking, G. *Dalton Trans.* **2001**, 434. (e) Uddin, J.; Frenking, G. *J. Am. Chem. Soc.* **2001**, *123*, 1683. (f) Boehme, C.; Uddin, J.; Frenking, G. *Coord. Chem. Rev.* **2000**, *197*, 249. (g) Xu, L.; Li, Q.-S.; Xie, Y.; King, R. B.; Schaefer, H. F. *Inorg. Chem.* **2010**, *49*, 1046. (h) Pandey, K. K.; Musaev, D. G. *Organometallics* **2010**, *29*, 142.

(5) Ehlers, A. W.; Baerends, E. J.; Bickelhaupt, F. M.; Radius, U. *Chem.—Eur. J.* **1998**, *4*, 210.

 Published on Web 08/16/2010

borylenes possess improved σ-donor and π-acceptor properties, thus leading to increased thermodynamic stability of the coordination products with respect to homolytic cleavage of the metal-borylene multiple bond.[5]

Since the most general approach to group 6 terminal borylene complexes $[(OC)_5M{=}B{=}N(SiMe_3)_2]$ (M = Cr **2b**, W **2c**) was reported in 1998[6] and subsequently extended to various central metals and boron bound substituents[7,3e] various of their reactivity patterns have been investigated.[3] Most notably, these compounds have turned out to be convenient sources for borylenes B−R (R = $N(SiMe_3)_2$) that could be efficiently transferred to suitable borylene acceptors under standard conditions. Thus, transmetalation of borylenes has been established,[8] as well as borylene transfer to unsaturated organic substrates such as alkenes[9] and alkynes[10] became possible for the first time. The latter, that is, the borylene based functionalization of carbon−carbon triple bonds, provides a facile access to borirenes, which are isoelectronic with cyclopropenium cations, and thus, constitute the smallest boron heterocycle that might exhibit 2π-aromatic stabilization.[11] Despite considerable fundamental interest in aromatic and antiaromatic unsaturated boron-containing heterocycles such as borirenes,[11] boroles,[12] and borepins,[13] only a limited number of synthetic routes to borirenes have been published,[2,11d,14] and among these, most are laborious and low yielding. Eisch et al. reported in 1987 the first structurally characterized borirene compound **1**, which was synthesized via photoisomerization of diaryl(arylethynyl)boranes (Scheme 1), and thus, provided experimental evidence, that is, shortened B−C and elongated C=C bond lengths, for the theoretically predicted Hückel aromaticity of this class of compounds.[14b,c] Nonetheless, the scope of synthetic approaches to borirenes is strongly limited with respect to the available substituents at the boron atom.

Scheme 1. Photoisomerization of Dimesityl(mesitylethynyl)borane in Donor Solvent

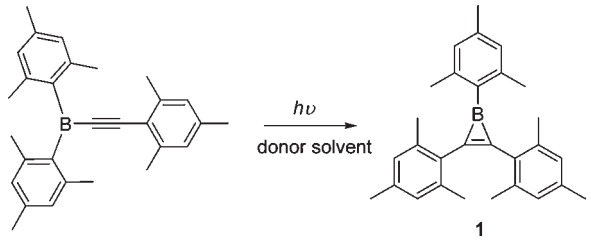

1

The borylene based functionalization of carbon−carbon triple bonds upon photolysis that we reported in 2005 provides a high yielding, straightforward access to borirene compounds.[10a] In our further studies, this has turned out to be applicable to a wide range of substrates such as alkynes, diynes[10b] (Scheme 2), and thus a variety of borirene compounds has been synthesized and fully characterized. The proposed aromaticity of borirenes and extensive π-delocalization over the BCC-ring has been confirmed by altered endocyclic bond lengths and a significantly decreased barrier to rotation about the exocyclic B−N double bond. This synthetic strategy gives access to a new class of boron-based π-conjugated systems with particularly interesting photophysical properties.[15] As the introduction of a metal center into the π-conjugated chain may introduce a range of different properties with regard to redox, magnetic, optical and electronic characteristics,[16] we recently reported the borylene based functionalization of σ−alkynyl complexes of platinum, which yielded such molecular frameworks involving d-block metals.[17]

Despite a somewhat broader range of well characterized borirenes our vision of reactivity of these three-membered

(6) Braunschweig, H.; Kollann, C.; Englert, U. *Angew. Chem.* **1998**, *110*, 3355. Braunschweig, H.; Kollann, C.; Englert, U. *Angew. Chem., Int. Ed.* **1998**, *37*, 3179.

(7) (a) Braunschweig, H.; Colling, M.; Kollann, C.; Merz, K.; Radacki, K. *Angew. Chem.* **2001**, *113*, 4327. Braunschweig, H.; Colling, M.; Kollann, C.; Merz, K.; Radacki, K. *Angew. Chem., Int. Ed.* **2001**, *38*, 4198. (b) Braunschweig, H.; Radacki, K.; Scheschkewitz, D.; Whittell, G. R. *Angew. Chem.* **2005**, *117*, 1685. Braunschweig, H.; Radacki, K.; Scheschkewitz, D.; Whittell, G. R. *Angew. Chem., Int. Ed.* **2005**, *44*, 1658 (VIP). (c) Blank, B.; Braunschweig, H.; Colling-Hendelkens, M.; Kollann, C.; Radacki, K.; Rais, D.; Uttinger, K.; Whittel, G. *Chem.−Eur. J.* **2007**, *13*, 4770.

(8) (a) Braunschweig, H.; Colling, M.; Kollann, C.; Neumann, B.; Stammler, H.-G. *Angew. Chem.* **2001**, *113*, 2359. Braunschweig, H.; Colling, M.; Kollann, C.; Neumann, B.; Stammler, H.-G. *Angew. Chem., Int. Ed.* **2001**, *40*, 2298. (b) Braunschweig, H.; Colling, M.; Hu, C.; Radacki, K. *Angew. Chem.* **2003**, *115*, 215. Braunschweig, H.; Colling, M.; Hu, C.; Radacki, K. *Angew. Chem., Int. Ed.* **2003**, *42*, 205. (c) Braunschweig, H.; Forster, M.; Radacki, K. *Angew. Chem.* **2006**, *118*, 8036. Braunschweig, H.; Forster, M.; Radacki, K. *Angew. Chem., Int. Ed.* **2006**, *45*, 2132. (d) Braunschweig, H.; Forster, M.; Radacki, K.; Seeler, F.; Whittell, G. *Angew. Chem.* **2007**, *119*, 5304. Braunschweig, H.; Forster, M.; Radacki, K.; Seeler, F.; Whittell, G. *Angew. Chem., Int. Ed.* **2007**, *46*, 5212. (e) Braunschweig, H.; Forster, M.; Kupfer, T.; Seeler, F. *Angew. Chem.* **2008**, *120*, 6070. Braunschweig, H.; Forster, M.; Kupfer, T.; Seeler, F. *Angew. Chem., Int. Ed.* **2008**, *47*, 5981.

(9) Braunschweig, H.; Dewhurst, R. D.; Herbst, T.; Radacki, K. *Angew. Chem.* **2008**, *120*, 6067. Braunschweig, H.; Dewhurst, R. D.; Herbst, T.; Radacki, K. *Angew. Chem., Int. Ed.* **2008**, *47*, 5978.

(10) (a) Braunschweig, H.; Herbst, T.; Rais, D.; Seeler, F. *Angew. Chem.* **2005**, *117*, 7627. Braunschweig, H.; Herbst, T.; Rais, D.; Seeler, F. *Angew. Chem., Int. Ed.* **2005**, *44*, 7461. (b) Braunschweig, H.; Herbst, T.; Rais, D.; Ghosh, S.; Kupfer, T.; Radacki, K.; Crawford, A.; Ward, R.; Marder, T.; Fern ndez, I.; Frenking, G. *J. Am. Chem. Soc.* **2009**, *131*, 8989. (c) Braunschweig, H.; Fernndez, I.; Frenking, G.; Radacki, K.; Seeler, F. *Angew. Chem.* **2007**, *119*, 5307. Braunschweig, H.; Fernndez, I.; Frenking, G.; Radacki, K.; Seeler, F. *Angew. Chem., Int. Ed.* **2007**, *46*, 5215.

(11) (a) Volpin, M. E.; Koreshkov, Y. D.; Dulova, V. G.; Kursanov, D. N. *Tetrahedron* **1962**, *18*, 107; For INDO calculations, see:. (b) Pittman, C. U.; Kress, A.; Patterson, T. B.; Walton, P.; Kispert, L. D. *J. Org. Chem.* **1974**, *39*, 373. (c) Allinger, N. L.; Siefert, J. H. *J. Am. Chem. Soc.* **1975**, *97*, 752; For ab initio calculations, see:. (d) Krogh-Jespersen, K.; Cremer, D.; Dill, J. D.; Pople, J. A.; Schleyer, P. v. R. *J. Am. Chem. Soc.* **1981**, *103*, 2589.

(12) (a) Eisch, J. J.; Hota, N. K.; Kozima, S. J. *J. Am. Chem. Soc.* **1969**, *91*, 4575. (b) Eisch, J. J.; Galle, J. E.; Kozima, S. *J. Am. Chem. Soc.* **1986**, *108*, 379. (c) Schleyer, P. v. R.; Freeman, P. K.; Jiao, H.; Goldfuss, B. *Angew. Chem. Int. Ed.* **1995**, *34*, 337. (d) Braunschweig, H.; Fernández, I.; Frenking, G.; Kupfer, T. *Angew. Chem.* **2008**, *120*, 1977. Braunschweig, H.; Fernández, I.; Frenking, G.; Kupfer, T. *Angew. Chem., Int. Ed.* **2008**, *47*, 1951. (e) Braunschweig, H.; Kupfer, T. *Chem. Commun.* **2008**, 4487. (f) Braunschweig, H.; Chiu, C.-W.; Radacki, K.; Brenner, P. *Chem. Commun.* **2010**, 916.

(13) (a) Eisch, J. J.; Galle, J. E. *J. Am. Chem. Soc.* **1975**, *97*, 4436. (b) Ashe, A. J., III; Drone, F. J. *J. Am. Chem. Soc.* **1987**, *109*, 1879. (c) Sugihara, Y.; Yagi, T.; Murata, I.; Imamura, A. *J. Am. Chem. Soc.* **1992**, *114*, 1479. (d) Ashe, A. J., III; Kampf, J. W.; Klein, W.; Rousseau, R. *Angew. Chem.* **1993**, *105*, 1112. Ashe, A. J., III; Kampf, J. W.; Klein, W.; Rousseau, R. *Angew. Chem., Int. Ed.* **1993**, *32*, 1065. (e) Schulman, J.; Disch, R. L. *Organometallics* **2000**, *19*, 2932. (f) Mercier, L. G.; Piers, W. E.; Parvez, M. *Angew. Chem., Int. Ed.* **2009**, *48*, 6108.

(14) (a) Pues, C.; Berndt, A. *Angew. Chem.* **1984**, *96*, 306. Pues, C.; Berndt, A. *Angew. Chem., Int. Ed. Engl.* **1984**, *23*, 313. (b) Eisch, J. J.; Shafii, B.; Rheingold, A. L. *J. Am. Chem. Soc.* **1987**, *109*, 2526. (c) Eisch, J. J.; Shafii, B.; Odom, J. D.; Rheingold, A. L. *J. Am. Chem. Soc.* **1990**, *112*, 1847.

(15) (a) Matsumi, N.; Chujo, Y. In *Contemporary Boron Chemistry, Spec. Publ. No. 253*; Davidson, M. G., Hughes, A. K., Marder, T. B., Wade, K., Eds.; Royal Society of Chemistry: Cambridge, 2000; pp 51−58; (b) Entwistle, C. D.; Marder, T. B. *Angew. Chem.* **2002**, *114*, 3051. Entwistle, C. D.; Marder, T. B. *Angew. Chem.* **2002**, *41*, 2927. (c) Jäckle, F. *J. Inorg. Organomet. Polym. Mater.* **2005**, *15*, 293. (d) Gabel, D. In *Science of Synthesis: Houben-Weyl Methods of Molecular Transformation*; Kaufmann, D., Matteson, D. S., Eds.; Verlag G. T. Thieme: Stuttgart, 2005; Vol. *6*, p 1277.

(16) Long, N. J.; Williams, C. K. *Angew. Chem.* **2003**, *115*, 2690. Long, N. J.; Williams, C. K. *Angew. Chem., Int. Ed.* **2003**, *42*, 2586.

(17) Braunschweig, H.; Ye, Q.; Radacki, K. *Chem. Commun.* **2009**, 6979.

Scheme 2. Borylene Based Functionalization of Alkynes, Diynes, and σ−alkynyl Complexes of Platinum upon Photolysis

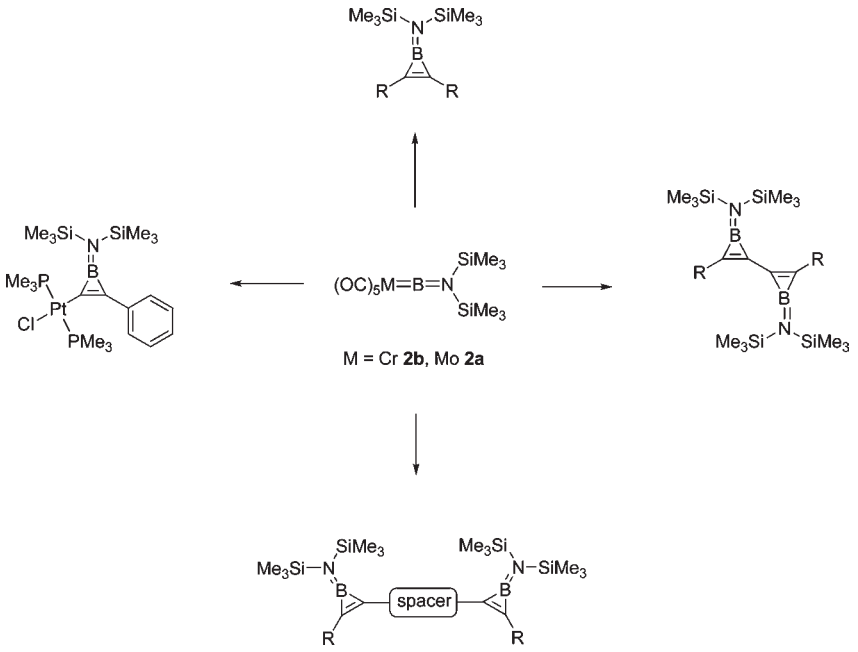

Scheme 3. Synthesis of the Iron-Substituted Borirene **4**

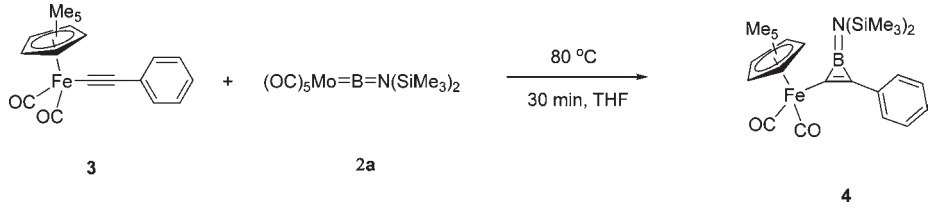

rings is still very limited and restricted to ring-opening with cleavage of one endocyclic B−C bond, initiated by either protic reagents, for example, water, methanol, or ethanol as reported already by Eisch et al.[14b,c] or by hydroboration with 9-borabicyclo-[3.3.1]nonane (9-BBN) as recently shown in our laboratory.[18] In addition, the above-mentioned transfer reaction requires activation by UV-light, thus strongly limiting its scope of application to photostable substrates.

Herein we report a thermally induced chemoselective borylene transfer from $[(OC)_5Mo{=}BN(SiMe_3)_2]$ (**2a**) to the carbon−carbon triple bond of an iron dicarbonyl alkynyl complex $[(\eta^5\text{-}C_5Me_5)Fe(CO)_2C{\equiv}CPh]$ (**3**), in which the iron atom acts as a competitive borylene acceptor. In addition an unprecedented reversible transformation between an iron-borirene and iron-boryl complex is described.

Results and discussions

Synthesis and Characterization of $[(\eta^5\text{-}C_5Me_5)(OC)_2Fe\{\mu\text{-}BN(SiMe_3)_2C{=}C\}Ph]$ (4) by Thermally Induced Borylene Transfer from $[(CO)_5Mo{=}B{=}N(SiMe_3)_2]$ (2a). As shown in Scheme 3, reaction of a pale yellow solution of $[(OC)_5Mo{=}B{=}N(SiMe_3)_2]$ (**2a**) with an equimolar amount of iron-alkynyl **3** in tetrahydrofuran (THF) at 80 °C yielded, within 30 min, the iron-substituted borirene complex (**4**). The reaction was monitored by ^{11}B NMR spectroscopy that revealed a complete conversion of the borylene complex **2a** (δ = 89.1 ppm) into the iron borirene species **4** (δ = 36.1 ppm). This result is in sharp contrast to initial experiments that we conducted under photochemical conditions. Here, we attempted to obtain **4** by irradiating an equimolar mixture of **3** and the chromium borylene complex $[(CO)_5Cr{=}B{=}N(SiMe_3)_2]$ (**2b**) in toluene or THF in analogy to previously observed borylene transfer reactions to alkynes.[10] However, in contrast to these clean and selective reactions, photolysis of **2b** with **3** gave intractable mixtures of various boron containing species (vide infra). According to Scheme 3 though, the iron borirene **4** was isolated as a yellow, moderately air- and moisture sensitive solid material in sufficient yield (63%) after work up. Multinuclear NMR spectra of **4** were unobtrusive, displaying all relevant signals in the expected range, with the exception of those of the boron bound carbon atoms that were not observed because of quadrupolar coupling, thus confirming its constitution in solution. Most notably, ^1H NMR spectra revealed a single resonance at δ = 0.32 ppm for the nitrogen-bound $SiMe_3$ groups, thus indicating rapid rotation around the B−N bond at room temperature. This finding implies the presence of 2π-aromatic stabilization within the BCC-ring that reduces the B−N π-contribution, as observed before in related systems.[10,14b,c]

Single crystals of **4** suitable for X-ray diffraction analysis were obtained from a hexane solution at −60 °C. The molecule crystallizes in the monoclinic space group

(18) Braunschweig, H.; Herbst, T.; Radacki, K.; Frenking, G.; Celik, M. A. *Chem.—Eur. J.* **2009**, *15*, 12099.

Scheme 4. Irradiation of the Iron-Substituted Borirene **4**

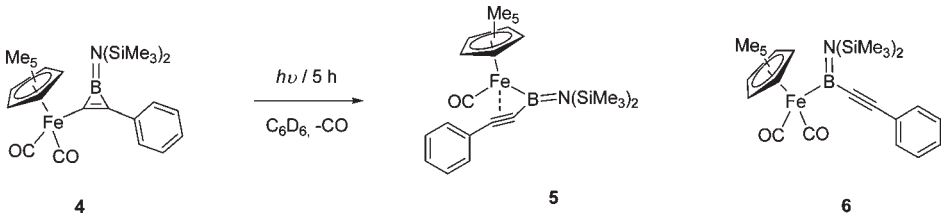

4 **5** **6**

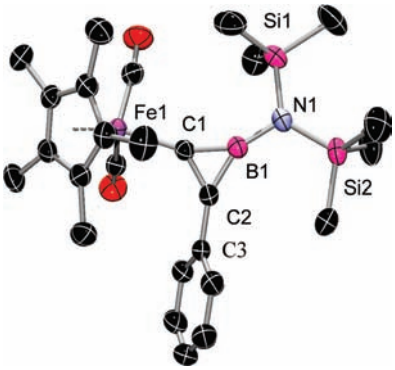

Figure 1. Molecular structure of **4.** Relevant bond lengths [Å] and angles [deg]: Fe1−C1 1.9826(14), C1−C2 1.3631(19), C1−B1 1.501(2), C2−B1 1.474(2), C2−C3 1.4699(19), B1−N1 1.4319(19), N1−Si1 1.7517(13), N1−Si2 1.7464(13), Fe1−C1−C2 137.60(10), C1−C2−C3 140.19(13), B1−C1−C2 61.73(10), B1−C2−C1 63.76(10), C1−B1−C2 54.52(9), C1−B1−N1 152.29(14), C2−B1−N1 153.03(15), B1−N1−Si1 112.67(10), B1−N1−Si2 121.10(10).

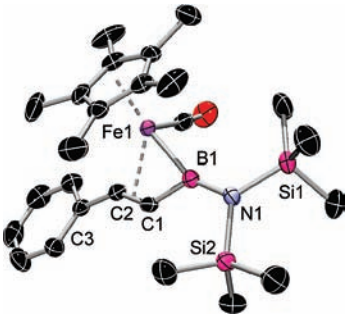

Figure 2. Molecular structure of **5**. Relevant bond lengths [Å] and angles [deg] for one of two independent molecules in the asymmetric unit, which feature very similar structures: Fe1−B1 1.9950(17), B1−N1 1.403(2), B1−C1 1.521(2), C1−C2 1.268(2), C2−C3 1.453(2), Fe1−B1−N1 153.59(12), C1−B1−N1 135.14(14), Fe1−B1−C1 71.09(9), B1−C1−C2 133.98(14), C1−C2−C3 147.34(15), B1−N1−Si1 123.20(10), B1−N1−Si2 114.42(10), Si1−N1−Si2 121.66(7).

*P*2(1)/*c* and displays the overall geometry of an aminoborirene. In particular, the endocyclic distances, that is, C1−C2 1.3631(19) Å, C1−B1 1.501(2) Å, C2−B1 1.474(2) Å together with the slightly elongated B−N separation of 1.4319(19) Å resemble that of previously reported borirenes with exocyclic B−N bonds (Figure 1). These data are in accord with extensive delocalization of the two π-electrons over a three-center bonding molecular orbital composed of the p-atomic orbitals of boron and carbon. The phenyl ring and the boracyclopropene unit are not coplanar, but enclose a dihedral angle of 67.03°, which is presumably due to steric congestion imposed by the bulky $N(SiMe_3)_2$ groups and the Cp*-ligand (Cp* = η^5-C_5Me_5). The distance of 1.9826(14) Å between Fe1 and the sp^2-hybdrized C1 is somewhat greater as the corresponding bond in the alkynyl precursor **3** (1.924(7) Å), where the C1-atom is sp-hybdrized,[19] and is thus comparable with the Fe−C bond in [Cp*Fe$(CO)_2$-C_6F_5] (Cp* = η^5-C_5Me_5) (1.970(4) Å),[20] which connects the iron center to an aromatic ring.

Irradiation of [(η^5-C_5Me_5)$(OC)_2$Fe{μ-BN$(SiMe_3)_2$C=C}-Ph] (4). Because of the aforementioned preliminary results on the attempted photochemical synthesis of **4**, we became interested in the behavior of this borirene complex upon irradiation with UV light. Room temperature photolysis of a yellow C_6D_6 solution of **4** was carried out in a sealed Young-NMR-tube. The reaction was monitored by ^{11}B NMR spectroscopy, which revealed gradual consumption of the starting material **4** and formation of two new boron-containing compounds **5** and **6** in a ratio of approximately 3:1, as indicated by new resonances at δ = 75.5 and 86.7 ppm respectively. After full characterization of these new compounds (vide infra) it became obvious that the formation of a mixture is due to the incomplete ejection of CO imposed by the closed reaction vessel. Thus, we irradiated **4** under similar conditions, but replaced the atmosphere in the NMR tube every 30 min by dry argon, which led to complete conversion of **4** into **5** as evidenced by ^{11}B NMR spectroscopy (Scheme 4). After work up, complex **5** was isolated as a red, moderately air- and moisture sensitive solid in 71% yield.

The significant downfield shift in the ^{11}B NMR spectrum of **5** in comparison to **4** of approximately 40 ppm already indicates a rearrangement of the former borirene moiety, as such deshielded resonances are typically found for iron bound boryl groups.[21] Additionally, the observation of two broad signals for the nitrogen-bound trimethylsilyl groups at 0.58 and 0.43 ppm in a 1:1 ratio at ambient temperature in the ^{1}H NMR spectrum indicates a significantly increased rotational barrier of the nitrogen−boron bond. These spectroscopic data are in good accordance with the molecular structure of **5** as elucidated in the crystal, in which the B−N π-contribution is increased as a result of the BCC-ring-opening.

Single crystals of **5** suitable for X-ray crystallography were obtained by cooling a hexane solution to −60 °C. The molecule crystallizes in the triclinic space group $P\bar{1}$ with two almost identical molecules in the asymmetric unit. As the geometry of both subunits is identical within the experimental error, only one set of data will be discussed in the following. As shown in Figure 2, the overall

(19) Akita, M.; Terada, M.; Oyama, S.; Morooka, Y. *Organometallics* **1990**, *9*, 816.

(20) Chukwu, R.; Hunter, A. D.; Santarsiero, B. D.; Bott, S. G.; Atwood, J. L.; Chassaignac, J. *Organometallics* **1992**, *11*, 589.

(21) (a) Braunschweig, H.; Ganter, B.; Koster, M.; Wagner, T. *Chem. Ber.* **1996**, *129*, 1099. (b) Braunschweig, H.; Kollann, C.; Englert, U. *Eur. J. Inorg. Chem.* **1998**, 465. (c) Braunschweig, H.; Kollann, C.; Müller, M. *Eur. J. Inorg. Chem.* **1998**, 291. (d) Hartwig, J. F.; Huber, S. *J. Am. Chem. Soc.* **1993**, *115*, 4908.

Scheme 5. Synthesis of **6** upon Carbonylation of **5**

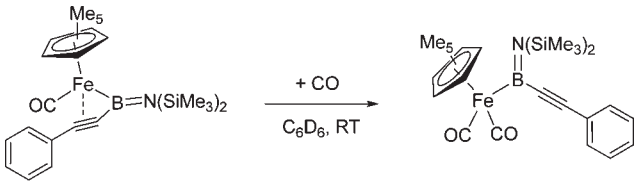

5 6

appearance of **5** is that of an (alkynyl)boryl complex, in which the boron bound C−C triple bond coordinates in a η^2-fashion to the iron center, thus constituting a highly unusual structural motif in boryl chemistry. While the sum of angles around boron B1 (359.82°) and nitrogen N1 (359.28°) proves planar coordination for both atoms, the Fe1−B1−C1 angle of 71.09°(9) displays significant deviation from ideal trigonal planar geometry commonly observed for sp^2-hybdrized boron centers, thus indicating a highly strained molecular structure. Likewise, the Fe1−B1 separation of 1.9950(17) Å is rather short for a iron-boryl bond and matches, for example, the one in $[(\eta^5\text{-}C_5H_5)(OC)_2Fe{-}B(F){-}Si(SiMe_3)_3]$ (1.983(9) Å), despite the fact that the latter is sterically less congested because of the presence of the parent C_5H_5 ligand at the iron center.[22] The side-on coordination of the alkynyl group has the expected effect on the C−C triple bond. Thus, the C1−C2 distance, which amounts to 1.268(2) Å is significantly elongated in comparison to the non-coordinated C−C triple bond in **6** (1.208(3) Å; vide infra), but very similar to values typically found for alkynes that are η^2-coordinated to a metal of the iron triad.[23] The overall geometry of the C3−C2−C1−B1 moiety gives further evidence for the presence of molecular strain, as the boryl- and the phenyl group adopt a mutual *trans* disposition with respect to the C1−C2 multiple bond displaying angles of 147.34(15)° (C1−C2−C3) and 133.98(14)° (B1−C1−C2), respectively. Finally, the somewhat shortened B−N bond length of 1.403(2) Å in comparison to the value of 1.4319(19) Å found for the borirene complex **4** indicates a slightly stronger π-interaction between boron and the exocyclic nitrogen atom because of cleavage of the BCC-ring and canceling of the endocyclic 2 π electron delocalization.

$[(\eta^5\text{-}C_5Me_5)(OC)_2FeBN(SiMe_3)_2CCPh]$ (6). To provide selective access to the dicarbonyl complex **6**, the previously obtained monocarbonyl species **5** was treated with CO. To this end, a deep red solution of **5** in C_6D_6 was kept under an atmosphere of CO at ambient temperature for a couple of hours (Scheme 5). The progress of reaction was monitored by multinuclear NMR spectroscopy, which revealed gradual consumption of the starting material **5**, and quantitative formation of a new boron containing compound as indicated by the presence of a new resonance at δ = 86.7 ppm in the ^{11}B NMR spectrum. After work up, **6** could be isolated by crystallization from hexanes at −60 °C as an analytically pure, tawny crystalline solid in 52% yield.

The spectroscopic data of **6** in solution are in agreement with the proposed structure. In particular, the aforementioned deshielded ^{11}B NMR resonance of δ = 86.7 ppm indicates the presence of a metal bound boryl ligand. Interestingly, the ^{1}H NMR spectrum at ambient temperature shows only one resonance at δ = 0.46 ppm for the nitrogen-bound $SiMe_3$ group, which suggests a reduced rotational barrier of the B−N bond in comparison with that in **5**. This finding is somewhat surprising as hindered rotation about B−N double bonds is well documented for both (amino)boryl complexes of the type $[(\eta^5\text{-}C_5R_5)(OC)_2Fe{-}B(NR_2)R']$[21b] and alkynyl(amino)boranes $R(R'_2N)B{-}C{\equiv}C{-}R'$.[24]

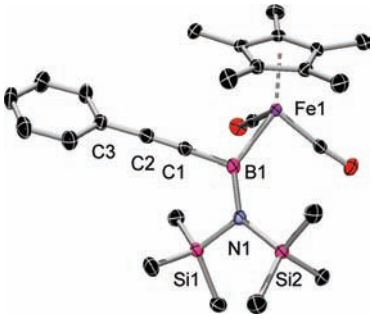

Figure 3. Molecular structure of **6.** Relevant bond lengths [Å] and angles [deg]: Fe1−B1 2.075(2), B1−C1 1.554(3), B1−N1 1.444(3), C1−C2 1.208(3), C2−C3 1.439(3), Fe1−B1−C1 111.64(13), Fe1−B1−N1 131.84(15), C1−B1−N1 115.83(16), B1−N1−Si1 115.97(13), B1−N1−Si2 125.21(13), Si1−N1−Si2 117.69(9), B1−C1−C2 178.4(2), C1−C2−C3 177.0(2).

The formation of **6** was further confirmed by X-ray diffraction analysis. Suitable single crystals were obtained from a hexane solution at −70 °C, and the molecule crystallizes in the orthorhombic space group *Pbca*. The major difference between **6** and **5** lies with the almost undistorted geometry of the boryl group in case of the former. As shown in Figure 3, the sum of the angles around boron B1 (359.3°) and nitrogen N1 (358.9°) prove planar coordination geometries for boron atoms. However, because of the "free" alkynyl group, the angles Fe1−B1−C1 (111.64(13)°), Fe1−B1−N1 (131.84(15)°), and C1−B1−N1 (115.83(16)°) indicate a non-strained, sp^2 hybridized boron atom. The Fe1−B1 separation of 2.075(2) Å is significantly larger than that in **5** and marks the higher end of Fe−B distances commonly observed for neutral iron half-sandwich boryl complexes of iron (196−209 ppm).[3d] Consistent with the results from ^{1}H NMR spectroscopy, the B−N bond length of 1.444(3) Å resembles that of the iron borirene complex **4** (1.4319(19) Å), and thus suggests a comparable B−N π-interaction.

Stepwise Transformation from 6 to 4 under Thermal Conditions. To evaluate the thermal stability of the unusual (alkynyl)boryl complex **6**, a tawny solution of this complex in C_6D_6 was heated at 80 °C under argon in a sealed Young-NMR-tube, and the reaction was monitored by multinuclear NMR spectroscopy. ^{11}B NMR spectra revealed a gradual consumption of **6** (δ = 86.7 ppm) with concomitant formation of **5** (δ = 75.5 ppm). However, as evidenced by a ^{11}B NMR signal at δ = 36.1 ppm and corresponding resonances in the ^{1}H NMR spectrum, a small amount of **4** was formed as well. Upon the assumption that part of the thermally dissociated CO was not

(22) Braunschweig, H.; Colling, M.; Kollann, C.; Englert, U. *J. Chem. Soc., Dalton Trans.* **2002**, 2289.
(23) Ball, R. G.; Burke, M. R.; Takats, J. *Organometallics* **1987**, *6*, 1918.
(24) Feulner, H.; Metzler, N.; Nöth, H. *J. Organomet. Chem.* **1995**, *489*, 51.

Scheme 6. Stepwise Transformation from **6** to **4** under Thermal Conditions

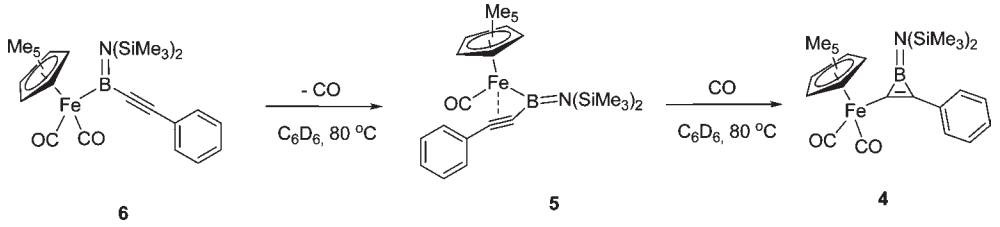

6 5 4

Scheme 7. Synthesis of Phosphane Complex **7**

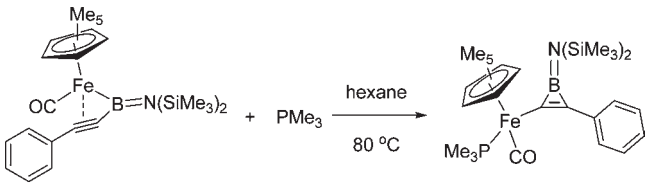

5 7

distributed into the gas phase and thus, enabled the formation of the borirene(dicarbonyl) complex **4**, we heated the reaction mixture under a dry atmosphere of CO. As indicated by the characteristic ^{11}B- (δ = 36.1 ppm) and ^{1}H NMR resonances (δ = 0.42 (s, 18H, Si(CH_3)$_3$), 1.42 (s, 15H, C_5(CH_3)$_5$)) the intermediate **5** was indeed completely converted into **4** under these conditions (Scheme 6).

The thermal conversion of the iron (alkynyl)boryl **6** into the iron borirene **4** is unprecedented in metal boryl/borirene chemistry and suggests that **4** is thermodynamically favored over **6** (vide infra). Morevover, **4** and **6** constitute a pair of hitherto unknown iron boron species, which are fully convertible under either photochemical or thermal conditions. Likewise interesting is the fact that the isomerization of an alkynylborane into a borirene (**1**) has been reported by Eisch et al.[14b,c] (Scheme 1), however, under photochemical conditions. Thus, the thermal reaction depicted in Scheme 6 constitutes a complementary synthetic approach to these boron heterocycles.

Synthesis of [(η^5-C_5Me_5)(OC)(PMe_3)Fe{μ-BN($SiMe_3$)$_2$-C=C}Ph] (7). Finally we investigated, whether the addition of CO to **5** at elevated temperature with isomerization into **4** can be extended to different ligands such as phosphines. As shown in Scheme 7, reaction of a deep red solution of **5** with an equimolar amount of PMe_3 in hexane at 80 °C yielded the phosphane complex **7** within 1 h. The reaction was monitored by multinuclear NMR spectroscopy, which revealed formation of a new boron- and phosphorus-containing compound, as indicated by the presence of a new resonance at δ = 38.4 ppm in the ^{11}B NMR spectrum, and at δ = 35.39 ppm in the ^{31}P NMR spectrum. The iron borirene derivative **7** was isolated in the form of yellow crystals by filtration of the reaction mixture and subsequent crystallization from hexanes at −70 °C.

Single crystals of **7** suitable for X-ray diffraction analysis were obtained from a hexane solution at −70 °C. The molecule crystallizes in the triclinic space group $P\bar{1}$, and the overall geometry resembles that of (Figure 4), in accord with extensive delocalization of the two π-electrons over a three-center bonding molecular orbital from the p-atomic orbitals of boron and carbon. Because of stronger σ-donor ability of the phosphane ligand, the

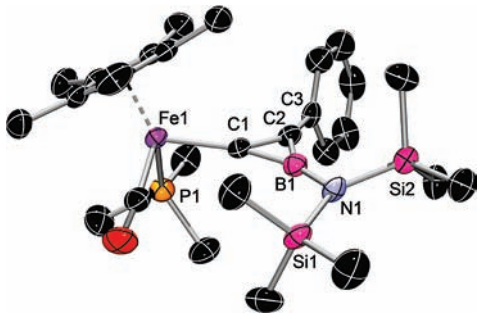

Figure 4. Molecular structure of **7.** Relevant bond lengths [Å] and angles [deg]: Fe1−C1 1.9727(16), Fe1−P1 2.1753(5), C1−C2 1.380(2), C1−B1 1.506(2), C2−B1 1.473(2), C2−C3 1.473(2), B1−N1 1.443(2), Fe1−C1−C2 142.59(12), N1−Si1 1.7491(13), N1−Si2 1.7475(14), Fe1−C1−B1 155.98(12), C2−C1−B1 61.21(11), C1−C2−B1 63.62(12), C1−C2−C3 143.45(15), C3−C2−B1 152.57(15), C1−B1−N1 156.17(15), C2−B1−N1 148.63(16), B1−N1−Si1 113.78(11), B1−N1−Si2 111.46(10), Si1−N1−Si2 134.23(8).

B1−C1, C1−C2, and B1−N1 bonds are slightly longer in comparison to those in **4**. The dihedral angle of 86.69° between the phenyl ring and the boracyclopropene unit is larger than in **4**, which may be due to the presence of the phosphane ligand and its higher sterical demand in comparison to CO.

Quantum Chemical Calculations. To understand the mechanisms of the experimentally observed reactions and to analyze the bonding situation in the molecules particularly in the unusual compounds **5** and **6** we optimized the geometries of **4**−**7** with quantum chemical methods using density functional theory (DFT) at the M052X/def2-SVP level of theory. Improved energies were obtained using larger basis sets at M052X/def2-TZVPP at M052X/def2-SVP optimized geometries. Figure 5 shows the calculated structures with the most important bond lengths and the relative energies of the molecules. The full set of geometrical parameters is given in the Supporting Information.

The calculated geometry of **4** is in excellent agreement with the results of the X-ray structure analysis (Figure 1). The differences between theory and experiment are within the expected error range of the theoretical method and may also arise from intermolecular interactions in the solid. A very good agreement between the calculated and experimental geometry is also found for the unusual compound **5**. It is interesting to note that the calculated interatomic distances Fe−C1 (2.088 Å) and Fe−C2 (2.087 Å) have nearly the same value which poses the question about the nature of the interactions between Fe and the C_2 moiety in **5**. Figure 6 shows the Laplacian distribution $\nabla^2\rho$(r) of the central moiety in **5** which addresses this question. There are bond paths between Fe−C2, C2−C1, C1−B, and Fe−B but there is no bond path

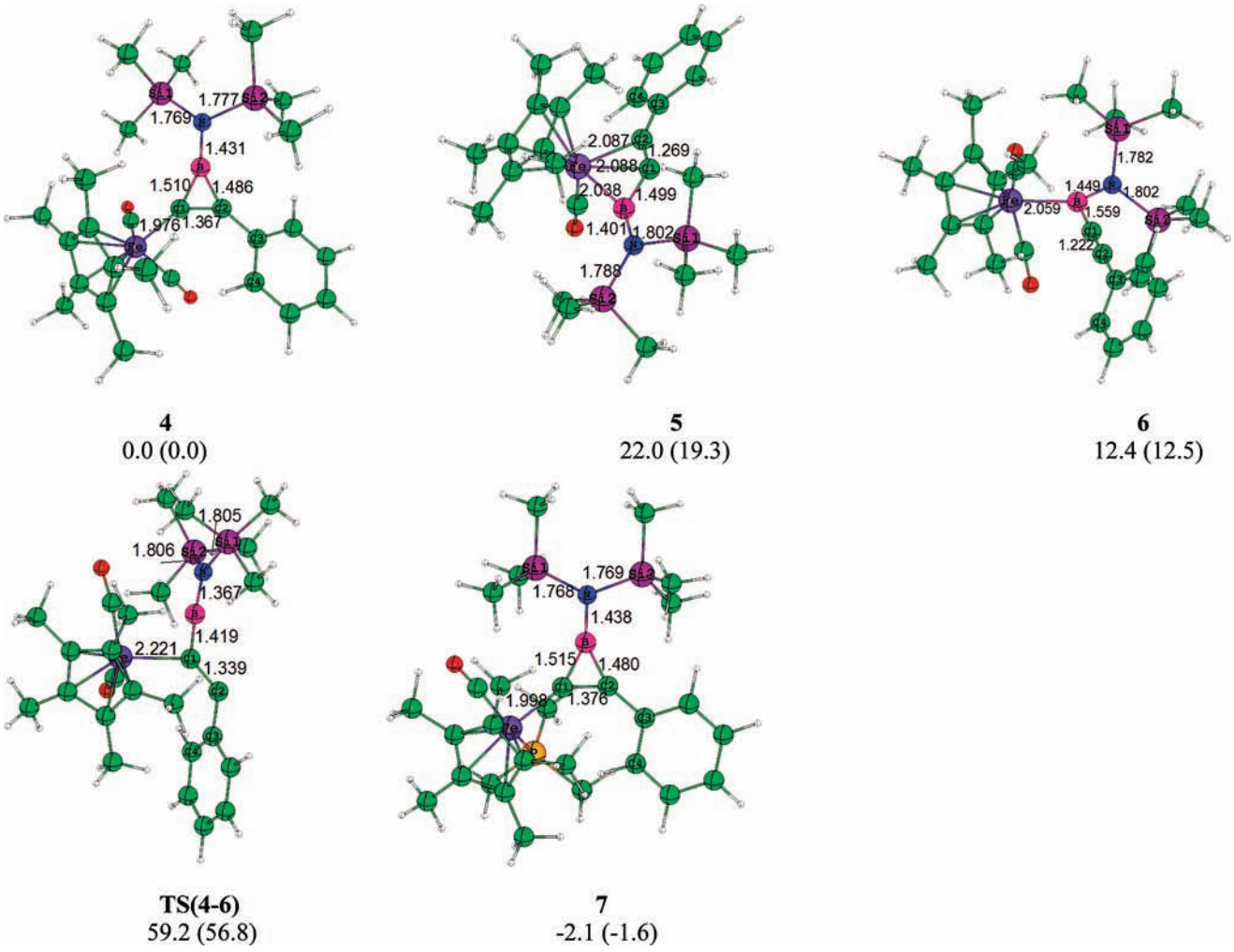

Figure 5. Optimized geometries (M052X/def2-SVP) and relative energies in kcal/mol (M052X/def2-TZVPP//M052X/def2-SVP) of the calculated molecules. The relative energies including ZPVE corrections at M052X/def2-SVP level are given in parentheses.

between Fe−C1. There is ring critical point for the FeC2C1B moiety which identifies it according to the AIM (Atoms in Molecules) criteria as a four-membered ring. Note that the carbon atom C2 has an area of charge concentration which has the shape of a droplet-like appendix pointing toward the Fe atom while there is no such feature in the Laplacian field of C1. We could locate a gradient path from the ring critical point to the Fe atom and to the midpoint of the C1−C2 moiety. The translation of this information into simple bonding schemes supports the writing with a dashed line as shown in Figure 2.

Figure 5 gives the relative energy of **5** + CO with respect to **4** (22.0 kcal/mol) which is the theoretically predicted bond dissociation energy (BDE) D_e of one CO ligand in **4** provided that **5** is the global energy minimum. The BDE after correcting for zero-point vibrational contributions is D_o = 19.3 kcal/mol. Compound **6** which is an isomer of **4** is 12.4 kcal/mol higher in energy. Thus, the BDE of one CO ligand in **6** is only D_e = 9.6 kcal/mol (D_o = 6.9 kcal/mol). The carbonylation reaction **5** + CO → **6** (Scheme 5) which slowly takes place at room temperature is thus calculated to be exothermic by 6.9 kcal/mol. We did not calculate transition states for the rotation about the B−N bonds in **5** and **6** but the latter compound (Figure 3) has a clearly longer bond (1.449 Å calc., 1.444(3) Å exper.) than the former molecule (1.401 Å calc., 1.403(2) Å exper.) which is in agreement with the NMR spectra suggesting that the rotational barrier in **6** is lower than in **5**.

The experimental observations which were described above indicate that **5** is formed from **6** via decarbonylation at 80 °C while the carbonylation of **5** under the same conditions gives **4** (Scheme 6). We were interested in the question if a direct rearrangement of the isomers **6** → **4** might be possible under thermal conditions. Therefore we calculated the transition state for the latter isomerization. The optimized transition state structure **TS(4−6)** is shown in Figure 5. The calculations predict that it is 59.2 kcal/mol higher in energy than **4** which means that the activation barrier for the reaction **6** → **4** is 46.8 kcal/mol. After correcting for zero-point vibrations we calculate a barrier of 44.5 kcal/mol. This is much higher than the decarbonylation/carbonylation reaction via **5**.

We also calculated the phosphane complex **7** (Figure 4) which is the product of the reaction **5** + PMe_3 (Scheme 7). Figure 5 shows the calculated geometry of **7** which is in very good agreement with the experimental values. The phosphane ligand effectuates slightly longer bonds in **7** for C1−C2, C1−B, and B−N while the C2−B bond is a bit shorter than in **4**. This trend reflects the experimental observations.

Table 1. Bond Orders *P* and Atomic Partial Charges *q* for Compounds **4**−**7**

no.	*P* Fe−C1	*P* Fe−C2	*P* Fe−B	*P* C1−C2	*P* C1−B	*P* C2−B	*P* B−N	*q* Fe	*q* C1	*q* C2	*q* B
4	0.76			1.68	1.04	1.02	0.98	−1.01	−0.19	−0.32	0.67
5	0.37	0.48	0.56	2.19	1.03		1.02	−0.82	−0.38	0.06	0.95
6			0.64	2.70	0.88		0.90	−1.30	−0.36	−0.02	0.96
7	0.76			1.65	1.04	1.04	0.97	−0.82	−0.23	−0.35	0.65

The relative energy of **7** (−2.1 kcal/mol) is given with respect to **4**-CO + PMe_3. The ligand exchange reaction is thus predicted to be exothermic by 2.1 kcal/mol (1.6 kcal/mol after ZPE correction) and the reaction **5** + PMe_3 → **7** + CO is exothermic by 24.1 kcal/mol (20.9 kcal/mol after ZPE correction) which is in agreement with the observed reaction course under thermal conditions.

We calculated the charge distribution and bond orders of compounds **4**−**7**. Table 1 shows that C1−C2 bond order in **6** clearly suggests a triple bond while **5** has a weakened triple bond because of the stronger conjugation with the boron atoms. The C1−B bond order in **5** (1.03) is clearly bigger than in **6** (0.88). Note that the former compound has rather small bond orders for Fe−C2 (0.48) and particularly for Fe−C1 (0.37) which according to the AIM results is not a chemical bond. Both values are significantly smaller than the Fe−C1 bond orders for **4** and **7** (0.76) which supports the interpretation of a donor−acceptor bond in **5** between the C_2 moiety and the iron atom. The boron atoms carries large positive charges of 0.67 e in **4** and 0.65 e in **7** which are even larger in **5** (0.95 e) and **6** (0.96 e). The Fe atom has always a large negative charge of ∼ −1.0 e. The calculated bond orders for the B−N bond in **5** (1.02) and **6** (0.90) also support a lower B−N rotational barrier in **6** compared with **5** (Figure 6).

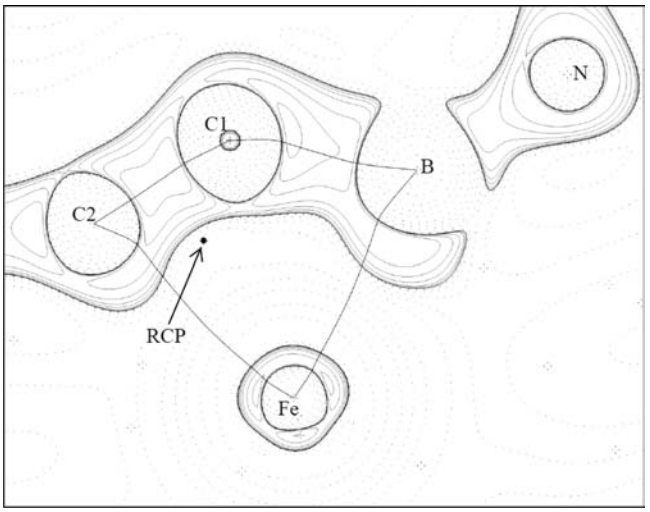

Figure 6. Contour line diagrams $\nabla^2\rho(r)$ of the central moiety in **5**. Solid lines indicate areas of charge concentration ($\nabla^2\rho(r) < 0$) while dashed lines show areas of charge depletion ($\nabla^2\rho(r) > 0$). Solid lines connecting atomic nuclei give the bond paths. The black dot indicates the ring critical point (RCP).

Conclusion

Here, we reported the selective synthesis of the iron borirene complex **4**, upon heating of the molybdenum borylene **2a** in the presence of the iron alkynyl complex **3**, thus establishing thermally induced borylene transfer for the synthesis of a metal borirene complex. Subsequently, we investigated the photochemical and thermal stability of the title compound and disclosed a fully reversible and unprecedented borirene-to-boryl transformation, which is summarized in Scheme 8.

In addition to full characterization of all new complexes **4**−**7** in solution and in the crystal, DFT calculations were performed, to elucidate the unusual electronic structure of **5** and to provide information about the thermodynamics of the aforementioned reversible transformations. Indeed, quantum chemical calculations suggest that the reaction **4**-CO → **5** is endothermic by 19.3 kcal/mol and that **6** is 12.4 kcal/mol higher in energy than **4**. The formation of the phosphane complex **7** in the reaction **5** +PMe_3 → **7** + CO is exothermic by 20.9 kcal/mol.

Experimental Section

General Procedures. All manipulations were performed either under dry argon or in vacuo using standard Schlenk line and glovebox techniques. Solvents (THF, ether, toluene, benzene and hexane) were purified by distillation under dry argon from appropriate drying agents (sodium and sodium wire, respectively) and stored under the same inert gas over molecular sieves. Carbon monoxide gas was previously passed through acetone-dry ice traps to remove moisture. NMR spectra were acquired on either a Varian Unity 500 (^{1}H: 499.834; ^{11}B: 160.364; ^{13}C: 125.697 MHz) or Bruker Avance 500 (^{1}H: 500.133; ^{11}B: 160.472; ^{13}C: 125.777 MHz) NMR spectrometer. ^{1}H and ^{13}C{^{1}H} NMR spectra were referenced to external TMS via the residual protio solvent (^{1}H) or the solvent itself (^{13}C). ^{11}B{^{1}H} NMR spectra were referenced to external $BF_3\cdot OEt_2$. ^{31}P{^{1}H} NMR spectra were referenced to 85% H_3PO_4. Microanalyses for C, H, and N were performed on either a Carlo Erba model 1106 or a Leco CHNS-932 Elemental Analyzer. PMe_3 was used as 0.10 mol·L^{-1} solution in hexane. $Na_2[M(CO)_5]$ (M = Cr, Mo),[25] $Cl_2B(SiMe_3)_2$,[26] iron alkynyl complex [(η^5-C_5Me_5)$(OC)_2$FeC≡CPh][19] and borylene complexes, $(OC)_5M$=$BN(SiMe_3)_2$ (M = Cr, Mo)[6] were prepared according to the literature. NMR spectroscopic experiments were performed in quartz or Young NMR tubes. The light source was a Hg/Xe arc lamp (400−550 W) equipped with IR filters, irradiating at 210−600 nm. Large-scale experiments were performed in a 150 mL Schlenk flask equipped with a quartz cooling jacket into which a Hg lamp (125 W) was inserted vertically.

Synthesis of [(η^5-C_5Me_5)$(OC)_2$Fe{μ-BN$(SiMe_3)_2$C=C}Ph] (4). In a Young NMR tube, a yellow solution of **2** (104 mg, 0.30 mmol) and **3** (120 mg, 0.30 mmol) in 2 mL of THF was heated in a oil bath at 80 °C for 0.5 h. The volatile components were removed in vacuo, and the brown residue was extracted with 5 mL of hexane. The brown hexane solution was stored at −60 °C overnight to separate $Mo(CO)_6$. The filtrate was stored at −60 °C for 2 weeks to afford yellow crystals of **4** (98 mg, 63% yield). ^{1}H NMR: δ = 0.42 (s, 18H, Si(CH_3)$_3$), 1.42 (s, 15H, C_5(CH_3)$_5$), 7.09 (m, 1H, C*H*-*p* of C_6H_5), 7.31 (m, 2H, C*H*-*m* of C_6H_5), 7.47(m, 2H, C*H*-*o* of C_6H_5); ^{13}C{^{1}H}-NMR: (*C* bonded to boron not detected), δ = 217.76 (s, *C*O), 143.67 (s, *C* of C_6H_5), 128.53 (s, *C*H-*m* of C_6H_5), 126.21 (s, *C*H-*o* of C_6H_5), 125.69 (s, *C*H-*p* of C_6H_5), 96.21 (s, *C* of $C_5(CH_3)_5$), 9.93 (s, *C*H$_3$

(25) Maher, J. M.; Beatty, R. P.; Cooper, N. J. *Organometallics* **1985**, *4*, 1354.
(26) Haubold, W.; Kraatz, U. Z. *Anorg. Allg. Chem.* **1976**, *421*, 105.

Scheme 8. Synthesis of the Iron-Substituted Borirene **4**, Stepwise Reversible Metal-boryl(**6**)-to-borirene(**4**) Transformation and Synthesis of **7** upon the Unprecedented Metal-boryl-to-borirene Transformation

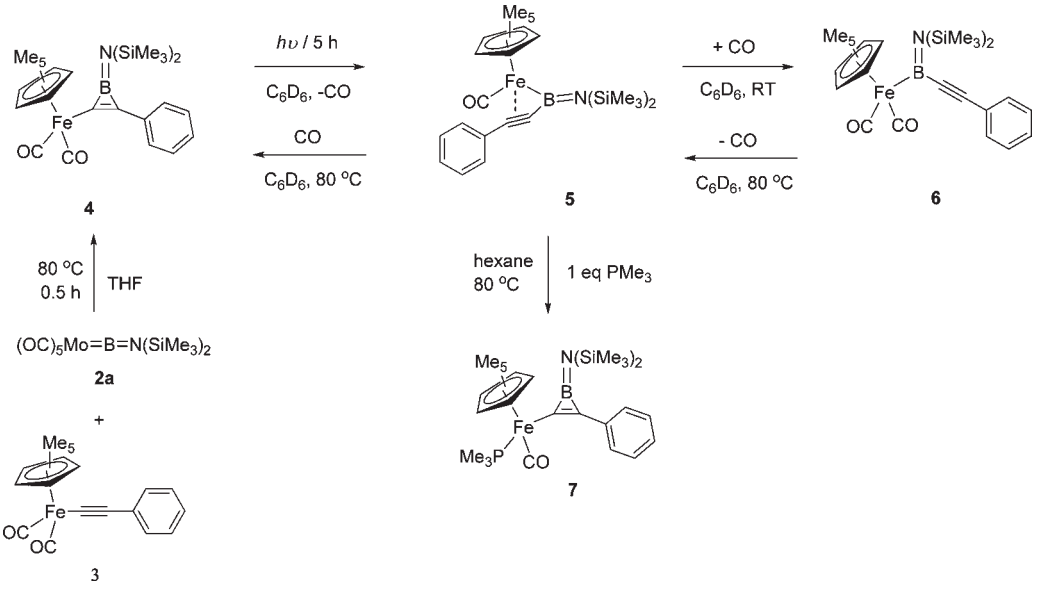

of $C_5(CH_3)_5$), 3.54 (s, Si(CH_3)$_3$); $^{11}B\{^1H\}$-NMR: δ = 36.1 (s). Elemental analysis calcd. [%] for $BC_{26}FeH_{38}NO_2Si_2$: C 60.12, H 7.37, N 2.70; found: C 59.96, H 7.35, N 2.94.

Synthesis of [(η^5-C_5Me_5)(OC)FeBN(SiMe$_3$)$_2$(η^2-CC)Ph] (5). In a 5 mm quartz NMR tube, a pale yellow solution of **4** (80 mg, 0.15 mmol) in 1 mL of C_6D_6 was irradiated for 4 h at room temperature. During this period the NMR tube was degassed and filled with fresh argon every half an hour. The volatile components were removed in vacuo, and the deep red residue was extracted with hexane. The concentrated filtrate was stored at −30 °C for several days to afford red crystals of **5** (54 mg, 71%). ^{1}H NMR: δ = 1.59 (s, 15H, $C_5(CH_3)_5$), 0.58 (bs, 9H, Si(CH_3)$_3$), 0.43 (bs, 9H, Si(CH_3)$_3$), 7.08 (m, 1H, C*H*-*p* of C_6H_5), 7.21 (m, 2H, C*H*-*m* of C_6H_5), 7.96(m, 2H, C*H*-*o* of C_6H_5); $^{13}C\{^1H\}$-NMR: (*C* of the alkyne ligand not detected), δ = 220.22 (s, *C*O), 133.08 (s, *C* of C_6H_5), 128.53 (s, *C*H-*m* of C_6H_5), 131.45 (s, *C*H-*o* of C_6H_5), 127.56 (s, *C*H-*p* of C_6H_5), 92.12 (s, *C* of $C_5(CH_3)_5$), 4.31 (bs, Si(CH_3)$_3$), 3.51 (bs, Si(CH_3)$_3$); $^{11}B\{^1H\}$-NMR: δ = 75.5; Elemental analysis calcd. [%] for $BC_{25}FeH_{38}NOSi_2$: C 61.10, H 7.79, N 2.85; found: C 61.23, H 7.92, N 3.20.

Synthesis of [(η^5-C_5Me_5)(OC)$_2$FeBN(SiMe$_3$)$_2$CCPh] (6). In a Young NMR tube, a deep red solution of **5** (40 mg, 0.08 mmol) in 1 mL of C_6D_6 was degassed and refilled with dry CO gas. A gradual color change from deep red to golden-brown could be observed. After keeping the reaction mixture under CO for 2 h, the volatile components were removed in vacuo, and the brown residue was extracted with 1.5 mL of hexane. The brown hexane solution was stored at −70 °C for a few days to afford yellow crystals of **6** (22 mg, 52% yield). ^{1}H NMR: δ = 0.68 (s, 18H, Si(CH_3)$_3$), 1.78 (s, 15H, $C_5(CH_3)_5$), 7.11 (m, 1H, C*H*-*p* of C_6H_5), 7.17 (m, 2H, C*H*-*m* of C_6H_5), 7.627(m, 2H, C*H*-*o* of C_6H_5); $^{13}C\{^1H\}$-NMR: (*C* of carbon−carbon triple bond not detected), δ = 218.08 (s, *C*O), 125.25 (s, *C* of C_6H_5), 128.83 (s, *C*H-*m* of C_6H_5), 130.55 (s, *C*H-*o* of C_6H_5), 128.16 (s, *C*H-*p* of C_6H_5), 96.84 (s, *C* of $C_5(CH_3)_5$), 9.99 (s, *C*H$_3$ of $C_5(CH_3)_5$), 5.12 (s, Si(CH_3)$_3$); $^{11}B\{^1H\}$-NMR: δ = 86.7 (s). Elemental analysis calcd. [%] for $BC_{26}FeH_{38}NO_2Si_2$: C 60.12, H 7.37, N 2.70; found: C 60.17, H 7.28, N 3.26.

Transformation from 6 to 4. In a Young NMR tube, a tawny solution of **6** (20 mg, 0.04 mmol) in C_6D_6 under argon was heated in a oil bath at 80 °C for 2 h, yielding a deep red solution constituted by **5** and a small amount of **4**, as indicated by ^{11}B- and ^{1}H NMR spectroscopy. The reaction mixture was degassed and refilled with dry CO gas, brought again to 80 °C for another 2 h, examined by multinuclear NMR spectroscopy, which indicated the formation of **4**.

Synthesis of [(η^5-C_5Me_5)(OC)(PMe$_3$)Fe{μ-BN(SiMe$_3$)$_2$C=C}-Ph] (7). In a Young NMR tube, a deep red solution of **5** (20 mg, 0.04 mmol) and PMe_3 (0.40 mL, c = 0.10 mol·L^{-1}, 0.04 mmol) in 1 mL of hexane was heated in a oil bath at 80 °C for 1 h. The volatile components were removed in vacuo, and the brown residue was extracted with 1.5 mL of hexane. The brown hexane solution was stored at −70 °C for several weeks to afford yellow crystals of **7** (15 mg, 65% yield). ^{1}H NMR: δ = 0.42 (s, 18H, Si(CH_3)$_3$), 1.55 (s, 15H, $C_5(CH_3)_5$), 0.97 (d, 15H, $^2J_{H-P}$ = 8.8 Hz, PMe_3), 7.06 (t, H, C*H*-*p* of C_6H_5), 7.29 (m, 4H, C*H*-*m* and C*H*-*o* of C_6H_5); $^{13}C\{^1H\}$-NMR: (*C* bonded to boron not detected), δ = 221.90 (d, $^2J_{C-P}$ = 35.0 Hz, *C*O), 147.51 (s, *C* of C_6H_5), 127.94 (s, *C*H-*m* of C_6H_5), 125.62 (s, *C*H-*o* of C_6H_5), 124.42 (s, *C*H-*p* of C_6H_5), 92.05 (s, *C* of $C_5(CH_3)_5$), 19.30 (d, $^2J_{C-P}$ = 26.1 Hz, *C* of PMe_3), 10.61 (s, *C*H$_3$ of $C_5(CH_3)_5$), 3.70 (s, Si(CH_3)$_3$); $^{11}B\{^1H\}$-NMR: δ = 38.4 (s); $^{31}P\{^1H\}$-NMR: δ = 35.39 (s). Elemental analysis calcd. [%] for $BC_{28}FeH_{47}NOPSi_2$: C 59.26, H 8.35, N 2.47; found: C 59.12, H 8.31, N 2.62.

X-ray Structure Determinations. The crystal data of **4**, **5**, **6** and **7** were collected on a Bruker X8Apex diffractometer with a CCD area detector and multilayer mirror monochromated $Mo_{K\alpha}$ radiation. The structure was solved using direct methods, refined with the Shelx software package (Sheldrick, G. *Acta Crystallogr*. **2008**, *A64*, 112−122) and expanded using Fourier techniques. All non-hydrogen atoms were refined anisotropically. Hydrogen atoms were assigned to idealized positions and were included in structure factors calculations.

Crystal Data for 4. $C_{26}H_{38}BFeNO_2Si_2$, M_r = 519.41, orange block, 0.27 × 0.25 × 0.19 mm^3, monoclinic space group $P2_1/c$, a = 15.9329(4) Å, b = 8.3475(3) Å, c = 22.8808(7) Å, β = 110.2980(10)°, V = 2854.17(15) Å^3, Z = 4, ρ_{calcd} = 1.209 g·cm^{-3}, μ = 0.634 mm^{-1}, F(000) = 1104, T = 233(2) K, R_1 = 0.0377, wR^2 = 0.0998, 7105 independent reflections [$2\theta \leq 56.66°$] and 309 parameters.

Crystal Data for 5. $C_{25}H_{38}BFeNOSi_2$, M_r = 491.40, orange block, 0.26 × 0.14 × 0.12 mm^3, triclinic space group $P\bar{1}$, a = 7.2055(8) Å, b = 19.729(2) Å, c = 19.868(2) Å, α = 71.520(5)°, β = 83.681(5)°, γ = 85.313(5)°, V = 2659.2(5) Å^3, Z = 4, ρ_{calcd} = 1.227 g·cm^{-3}, μ = 0.674 mm^{-1}, F(000) = 1048, T = 100(2) K, R_1 = 0.0346, wR^2 = 0.0826, 11191 independent reflections [$2\theta \leq 53.58°$] and 581 parameters.

Crystal Data for 6. $C_{26}H_{38}BFeNO_2Si_2$, M_r = 519.41, yellow needle, 0.13 × 0.05 × 0.05 mm^3, orthorhombic space group *Pbca*, a = 8.0512(7) Å, b = 18.0246(14) Å, c = 38.492(3) Å, V = 5586.0(8) Å^3, Z = 8, ρ_{calcd} = 1.235 g·cm^{-3}, μ = 0.648 mm^{-1}, $F(000)$ = 2208, T = 100(2) K, R_1 = 0.0478, wR^2 = 0.0857, 6425 independent reflections [$2\theta \leq 55.28°$] and 309 parameters.

Crystal Data for 7. $C_{28}H_{47}BFeNOPSi_2$, M_r = 567.48, yellow plate, 0.60 × 0.20 × 0.10 mm^3, triclinic space group $P\bar{1}$, a = 8.9941(5) Å, b = 11.8876(6) Å, c = 15.4367(8) Å, α = 92.142(2)°, β = 98.880(2)°, γ = 109.052(2)°, V = 1534.54(14) Å^3, Z = 2, ρ_{calcd} = 1.228 g·cm^{-3}, μ = 0.643 mm^{-1}, $F(000)$ = 608, T = 100(2) K, R_1 = 0.0343, wR^2 = 0.0833, 6248 independent reflections [$2\theta \leq 52.76°$] and 330 parameters.

Crystallographic data have been deposited with the Cambridge Crystallographic Data Center as supplementary publication no. CCDC 774455−774458. These data can be obtained free of charge from The Cambridge Crystallographic Data Centre via www.ccdc.cam.ac.uk/data_request/cif.

Theoretical Methods. The DFT calculations have been carried out using the hybrid meta functional M05−2X[27] in conjunction with the def2-SVP basis set.[28] The optimized structures have been verified as energy minima by calculating the vibrational frequencies analytically. Single point calculations have been carried at M05−2X/def2-TZVPP level.[29] NBO analysis[30] was performed at M05−2X/def2-SVP optimized geometries at the M05−2X/def2-TZVPP level. The program package Gaussian03 was used throughout.[31] The AIM calculations were carried out using the program AIMPAC.[32]

Acknowledgment. This work was supported by the Deutsche Forschungsgemeinschaft (DFG).

Supporting Information Available: CIF file for **4**, **5**, **6**, and **7**, Cartesian coordinates and total energies of all calculated compounds. This material is available free of charge via the Internet at http://pubs.acs.org.

(27) Zhao, Y.; Schultz, N. E.; Truhlar, D. G. *J. Chem. Theory Comput.* **2006**, *2*, 364.
(28) Schäfer, A.; Horn, H.; Ahlrichs, R. *J. Chem. Phys.* **1992**, *97*, 2571.
(29) Weigend, F.; Ahlrichs, R. *Phys. Chem. Chem. Phys.* **2005**, *7*, 3297.
(30) Reed, A. E.; Curtiss, L. A.; Weinhold, F. *Chem. Rev.* **1988**, *88*, 899.
(31) Frisch, M. J. et al. *Gaussian 03*, Rev. D.01; Gaussian, Inc.: Wallingford, CT, 2004; For full reference, see the Supporting Information.
(32) Bader, R. F. W.; http://www.chemistry.mcmaster.ca/aimpac/imagemap/imagemap.htm.